Discussion Paper
Research Project on Renewable Energy Economics,
Graduate School of Economics, Kyoto University

# Gone with the COVID-19?
# An empirical study on trans-boundary air pollution between China and South Korea

19 April 2021

**Yimeng DU, Teng MA, Tao XU**

Graduate School of Economics, Kyoto University
Graduate School of Economics, Kyoto University
Business School, Hunan Normal University

# Does COVID-19 influence trans-boundary air pollution? Evidence from China and South Korea

**Yimeng DU, Teng MA, Tao XU**

Graduate School of Economics, Kyoto University
Graduate School of Economics, Kyoto University
Business School, Hunan Normal University

**Abstract**:

By using a vector autoregression model with exogenous variables (VAR-X), this study empirically estimated the trans-boundary impact of China's air pollutants on South Korea, and discussed whether any such trans-boundary effect was reduced due to the lock-down measures adopted for decelerating the coronavirus disease 2019 (COVID- 19) outbreak. Our findings show that South Korea's air pollution is partly affected by China, while domestic pollution emissions are the main source of the severe air conditions. Specifically, we find that SO2 pollutants in capital regions of South Korea mainly orients from Gyeonggi province, while the PM2.5 concentrations are mainly caused by pollutants in Seoul and Incheon city. On the other hand, we find that the trans-boundary impact did not only exist across the "China to South Korea" route. SO2 pollutants in South Korea are confirmed to have trans-boundary impact on pollutant level of China as well. In addition, our estimated results suggest that during the COVID-19 outbreak, the lock-down measures taken in China lead to a decrease in the trans-boundary impact of both PM2.5 and SO2 pollution, and enlarged the gap between effect of domestic pollutions and trans-boundary pollutions. Our study concludes that the lock-down measures taken to contain the spread of COVID-19 in China, can lead to the improvement of air quality in nearby countries.

**Keywords**: COVID-19, trans-boundary air pollution, domestic pollution transmission, VAR-X

# 1. Introduction

The crisis caused by coronavirus disease 2019 (COVID-19) has affected economic activities around the world. The COVID-19 pandemic forced governments to impose un- precedented measures, including restrictions on movement, social interaction, non-essential businesses and services, to decelerate the spread of the pandemic. Therefore, the pandemic ultimately resulted in large short-term economic losses and a decline in global economic activity (Anjum, 2020; Baldwin and Wederdi Mauro, 2020; Baker et al., 2020). Recent data released by National Aeronautics and Space Administration (NASA) and European Space Agency indicate that pollution in some of the epicenters of COVID-19, such as China, Italy, Spain, and the US, has decreased by up to 30% (Urrutia-Pereira, et al., 2020). Deb et al. (2020) conclude that containment measures may have led to a 15% decline in industrial pro- duction worldwide, and thus have resulted in an improved air quality. Nearly one-third of cities were locked down, and various types of economic activities were prohibited to reduce the potential risk of cross-infection in China. The weekly PM2.5 concentration is estimated to have been reduced by 17% in the locked down cities in China (He et al., 2020). Similarly, Zhang et al. (2021) conclude that the outbreak of COVID-19 lead to substantial decrease of $NO_x$ emission and air quality changes in China. The authors find 40.5% decrease of $NO_x$ emission and 12.5% decrease of surface PM2.5 in 2020 first quarter in East China. Simultaneously, $NO_2$ concentrations of South East of the UK is estimated to be decreased by an average of 14-38% as a result of the COVID-19 lockdown (Wyche, et al., 2021).

The East Asian region has been suffering from air pollution for decades, especially trans-boundary air pollution (Yim et al., 2019). Zhang et al. (2017) investigates transboundary health impacts of transported global air pollution and international trade, and find that about 12% premature deaths related to PM2.5 pollution in 2007, were related to air pollutants emitted in a region of the world other than that in which the death occurred. Due to the seriously degraded air quality caused by rapid industrialization and urbanization in China, the trans-boundary transmission of the country's air pollution has been widely discussed in recent years. Oh et al. (2015) presents an evidence which support that aerosols emitting in China play a major role in the occurrence of multi-day severe air pollution episodes in cold seasons in Seoul, South Korea. Kim (2019) estimates the effects of wind direction on ambient air quality in South Korea to provide insights into the impact of the long-range transmission of air pollutants from China. As a result, Kim finds that winds blowing in the southwest direction have the largest impact on South Korea's air pollution levels, which is consistent with the direction of the emissions from Shanghai that worsen South Korean pollution levels.

While trans-boundary air pollution from China in other East Asian countries, especially in South Korea was identified, potential reduction in such trans-boundary pollution caused by environmental protection efforts taken in China have yet to be fully understood. Therefore, in this study, we focus on empirically estimating the trans-boundary air pollution between China and South Korea, and discussing whether lock-down measures taken in China reduced pollution level in South Korea indirectly. The vector autoregression model with exogenous variables (VAR-X) allow us to investigate the existence of reciprocal reactions among the air pollution indicators of the two countries by controlling country-specific climate features. Transboundary air pollution with different characteristics is analyzed by observing two types of air pollution indicators: the concentration of $PM_{2.5}$ and sulfur dioxide ($SO_2$). Additionally, we investigated not only trans-boundary air pollution among countries, but also domestic air pollution transmissions among regions in capital area of South Korea.

The remainder of this paper is organized as follows: Section 2 describes the main causes of trans-boundary air pollution. Section 3 explains the sample selection and describes the air pollution indicators. The analysis frameworks for the simple VAR model and VAR-X models are described in Section 4. The estimated results and discussion are provided in Section 5. Finally, Section 6 presents our conclusions and discusses the implications of the research.

## 2. Background

Our hypothesis is based on the phenomenon of Asian dust, a meteorological event in which yellow dust clouds passing over China are carried eastward to South Korea by strong and stable westerly winds (Chun et al., 2001; Bishop et al., 2002; Jia and Ku, 2019). Asian dust usually occurs from March to May, but it also takes place irregularly during the winter months. Although the major components of yellow dust are sand and materials from the earth's crust, various industrial pollutants have also contributed to the dust problem. According to Altindag et al. (2017), the average daily $PM_{10}$ concentrations in South Korea significantly increase within three days of a yellow dust event. The dust particles and the strong winds underlying the Asian dust phenomenon can directly affect pollution levels. As Park et al. (2003) and Lee et al. (2007) document, in South Korea, the levels of major pollutants, such as $PM_{10}$, $SO_2$, and $NO_2$, are significantly elevated during the Asian dust periods. Choi et al. (2001) and Li et al. (2012) suggest that Asian dust brings with it China's man-made pollution as well as its by-products.

[Figure 1]

As shown in Figure 1, the major sources of the yellow dust that affects South Korea are the Gobi Desert, the Inner Mongolian Plateau, the Northeastern desert areas, and the Loess Plateau. Almost 50% of the yellow dust in South Korea comes directly from the Gobi Desert and the Inner Mongolian Plateau, and the path through the national capital region located in the northern area of China [1] This national capital region, which is also known as the Jing-jin-ji (JJJ) Metropolitan Region, includes the economic region surrounding the municipalities of Beijing, Tianjin, and Hebei. Extreme air pollution incidents occur frequently in China, especially in urban economic belts such as the JJJ region, the Pearl River region, and the Yangtze River region (Wang et al. 2014). For a long time, the JJJ region has been seriously affected by air pollution, with the annual average PM2.5 concentration reaching 93 μg/m$^3$ in 2015 (MOE, 2015), which is almost 10 times higher than the WHO standard[2]. Our hypothesis for this study is that the pollutants brought by the dust storms in South Korea come mainly from the JJJ region, and thus we chose this region as our study area.

On the other hand, the study area in South Korea was selected as the Seoul Capital Area (SCA), including the metropolitan areas of Seoul, Incheon, and Gyeonggi Province. The SCA region is located in the northwestern part of the country, on the coast of the Yellow Sea and about 592 miles east of the JJJ regions in China (Kim, 2019). In recent years, air pollution in capital cities in South Korea has become an increasing threat to local residents and the environment. According to research conducted by NASA, which observed air pollution trends worldwide, Seoul is among the cities with the worst air pollution (NASA, 2015). Seoul's PM2.5 concentration averaged 24.8 μg/m$^3$ in 2019, which is more than twice the WHO standard (World Air Report, 2019).

[1] Measures in the case of Yellow Dust, Seoul Metropolitan Government. <http://english.seoul.go.kr/policy/welfare-health-security/measures-in-case-of-yellow-dust/>, accessed on 8 January 2021.}.

[2] The WHO guideline for air quality with no health risk stipulates that the annual average concentration of PM2.5 ought not exceed 10 μg/m$^3$.

## 3. Sample selection and data description

### 3.1 Sample area selection

The capital areas of China and South Korea, which are also known as the JJJ and SCA regions, respectively, were selected to be the sample areas for this study. This is because, for the reasons described above, both the JJJ region and SCA region are located within the major route of Asian dust, which can carry industrial pollutants, passing over Northern China and heading towards South Korea. At the same time, these capital regions are also the regions experiencing the most severe air pollution in the two countries. Moreover, these two capital regions have also been adopted in previous studies that endeavored to analyze the air quality in China and South Korea (Sun, et al., 2018; Kim, 2019; Kim, et al., 2020). Additionally, in order to investigate the transmission of domestic air pollution inside the SCA region, we separated the capital area of South Korea into the Gyeonggi province, Incheon city, and Seoul City. Figure 2 shows the locations of JJJ region and SCA region in China and South Korea, separately.

[Figure 2]

### 3.2 Sample period selection

Our sample period for the main regression was limited to the first half of the fiscal years 2019 and 2020, which is between 1 January and 4 June[3].This sample period was selected because the Asian dust storm shows strong seasonality. Dust events are most frequent between March and May, and the occurrence of such events outside this period is significantly less frequent (Jia and Ku, 2019). The 2019 sample is defined as the pre COVID-19 sample and is compared to the post COVID-19 sample from 2020. This two-period estimation allowed us to control for any potential seasonal effects on the levels of air pollution, including differences in electricity demand, seasonal changes in monsoon and weather conditions, and economic fluctuations.

Our COVID-19 dataset was a collection of the COVID-19 data maintained by Our World in Data[4]. This dataset is updated daily and includes data on confirmed cases, deaths, and testing. Figure 3 illustrates the daily confirmed cases in China and South Korea during the post COVID-19 period. The confirmed cases in China rapidly increased from late January, peaking on 13 February 2020, and have been steadily declining since then. In South Korea, we saw that the coronavirus outbreak started from 20 February and peaked on 29 February 2020, with 909 daily confirmed cases, constituting a time lag of nearly a half month behind China.

[Figure 3]

### 3.3 Data for measuring actual air pollution

Our empirical analysis observed the daily concentrations of PM2.5 and SO2, collected from 106 monitoring stations covering the capital areas of China and South Korea, as indicators of air quality. These capital areas were the JJJ region, which includes Beijing, Tianjin, and Hebei Province in China, and the SCA region, including the metropolitan area of Seoul, Incheon, and Gyeonggi Province in South Korea. We aggregated the station level data to the “capital region" level and further combined them with weather variables, including the daily average amount of precipitation, wind speed, and temperature. The air quality indicator data, including the

[3] The Wuhan Municipal Health Commission reported a cluster of cases of pneumonia in Wuhan, China, on 31 December, 2019 (WHO, 2020). To balance the sample for two years, we define the spread of pandemic from 1 January 2020.

[4] Data available at <https://ourworldindata.org/coronavirus-source-data>, Retrieved August 8, 2020.

concentration of both PM2.5 and SO2, were collected from the World Air Quality Project database, and the weather data were obtained from the Global Historical Climatology Network of the U.S. National Oceanic and Atmospheric Administration.

As shown in Figure 4, the capital areas of the two countries experienced similar seasonal variations in PM2.5 concentrations, where the pollution levels reached their highest points during the winter season. In addition, we found that the PM2.5 concentration in the capital areas of China remained higher than in the SCA region of South Korea. On the other hand, compared to the equivalent periods in previous years, the turning point of PM2.5 emissions occurred earlier, and the levels of PM2.5 concentration have sharply decreased since the COVID-19 cases have been confirmed.

[Figure 4]

On the contrary, the relatively greater degree of volatility in the SO2 concentration in China is demonstrated in Figure 5. The sharp increase in SO2 emissions in the cold season may be due to the usage of central heating systems in Northern China[5]. Several existing studies indicate that winter heating, especially coal heating, is a major source accounting for high SO2 levels during the winter season in China (Xiao et al., 2015; Wang, et al., 2018). Compared to the same periods in previous years, the average level of SO2 concentration in both China and South Korea seemed to have largely decreased in 2020.

[Figure 5]

Table 1 contains descriptive statistics on the variables used in our analysis, adopting the JJJ region and SCA region as the sample area. The average PM2.5 concentration in the JJJ region of China was 124.6 μg/m$^3$ in the pre COVID-19 period, and this kind of pollution concentration dropped to 117.4 μg/m$^3$ in the post COVID-19 period. Similarly, the mean PM2.5 concentration in the SCA region of South Korea decreased from 99.03 μg/m$^3$ to 79.96 μg/m$^3$. We observed a similar decrease in air pollution levels in the post COVID-19 period by comparing the average SO2 concentration in the capital areas of China and South Korea.

[Table 1]

Table 2 includes the descriptive statistics on the variables used in the regression, separating the SCA region into the Gyeonggi province, Incheon city, and Seoul city as target areas. Averaged level of PM2.5 pollution in Gyeonggi province shows relatively higher concentration than the other areas in the SCA region. On the contrary, as shown by the mean value of SO2 pollutants, SO2 concentration in Gyeonggi province was relatively lower than that in Incheon and Seoul region. In specific in the pre COVID-19 period, the average SO2 concentration in Gyeonggi province was 89.72 μg/m$^3$, while that in Incheon and Seoul city was 82.01 μg/m$^3$ and 88.49 μg/m$^3$, separately. Simultaneously, we observed drops in the average level of air pollution indicators in the JJJ region, Gyeonggi province, Incheon city, and Seoul city in the post COVID-19 period.

[Table 2]

Before proceeding to the estimation of the model, we identify the appropriate methodology

[5] The Chinese government confine central heating to the northern part of the country, which includes regions above the Qinling Mountains and Huai River. The capital areas selected as our study area are also located in the central heating areas.

based on integration order of the variables. The Augmented Dickey-Fuller (ADF) (Dickey and Fuller, 1979) and Phillips-Perron (PP) (Phillips and Perron, 1988) unit root tests have the null hypothesis that the variable has a unit root, and the Kwiatkowski-Phillips-Schmidt-Shin (KPSS) (Kwiatkowski et al., 1992) null hypothesis is that the variable is stationary. Table 3 presents the ADF, PP, and KPSS tests for the variables in level. The results of these stationary tests reveal that the variables' order of integration is I(0) in levels, saying that all variables are stationary at their level form. It allows us to adopt the standard VAR framework in this study.

[Table 3]

## 4 Empirical Methodology

By adopting the VAR model, we were able to measure the reciprocal reactions among air pollution indicators in the two countries, as well as the lagged and persistent effects.
Additionally, the VAR model for multivariate time periods is able to help us identify such reciprocal reactions under different circumstances, and thus illustrate the impact of the lock-down measures on trans-boundary pollution transmission between countries.
Define $y\_t = (CAQ_t, KAQ_t)'$, where $CAQ_t$ and $KAQ_t$ illustrate two indicators of air pollutants, including $PM_{2.5}$ and $SO_2$ concentration in the capital areas of China and South Korea, respectively. The VAR models can be obtained with a lag period of $k$, which can be described as:

$$y_t = \alpha + \sum_{j=1}^{k} \beta_j y_{t-j} + \epsilon_t, \qquad (1)$$

where $\alpha = (\alpha_c, \alpha_k)'$ is the intercept vector, and $\epsilon_t = (\epsilon_{ct}, \epsilon_{kt})'$is the residual term.
Meanwhile, to control for climate factors that may also have affected the concentration of PM2.5 and SO2, VAR-X models were adopted by adding control variables $X_t = (X_{ct}, X_{kt})'$, including the daily average amount of precipitation, wind speed, and temperature in the studied capital areas in former equation:

$$y_t = \alpha + \sum_{j=1}^{k} \beta_j y_{t-j} + \theta_t X_t + \epsilon_t. \qquad (2)$$

where $\beta_j$ refers to the autoregressive coefficient matrix that captures system dynamics. The choice of the number of lags $k$ is based on the lag order selection statistics presented in Table 4. We find that the statistical results in Panel A of Table 4, three of the five criteria including the LR (likelihood ratio), the FPE (final prediction error), and AIC (Akaike's information criterion) statistics suggest the use of three lags for the PM2.5 regression. Similarly, the LR, FPE, and AIC statistics suggest the use of two lags for the $SO_2$ regression. Therefore, $k = 3$ was initially selected for the $PM_{2.5}$ estimation, and $k = 2$ was chosen for $SO_2$ estimation.

[Table 4]

## 5. Estimation Results

### 5.1 Granger causality test

Through the Granger causality test used with the simple VAR model, we were able to analyze the causal relationship of air pollution among numerous countries. Panel A in Table 5 shows that the null hypothesis, "CPM2.5 cannot Granger-cause KPM2.5" was rejected at the 1 \%

significance level. This result indicates that the PM2.5 concentration in China induced Granger-causality for South Korea's PM2.5 pollution, regardless of whether the COVID-19 outbreak existed.

[Table 5]

On the contrary, as shown in Panel B in Table 5, the causality test of the null hypothesis "CSO2 cannot be a Granger-cause KSO2" at the 1% significance level indicates that SO2 pollution in China is not responsible for South Korea's SO2 concentration. On the other hand, in the pre COVID-19 period, the SO2 concentration in South Korea was found to be a Granger-cause of SO2 concentration in China as well. These granger-causality test results illustrate that trans-boundary PM2.5 pollution from China to South Korea seems to have a greater impact than SO2 emissions. In addition, we found that the SO2 emissions in South Korea may also have exerted a transboundary impact on those of China.

## 5.2 Impulse response functions

The stability test results show that the established VAR system satisfied the required stability condition and that it could be relied upon to analyze the interactions among variables. Figures 5 and 6 outline the impulse response functions (IRFs) based on the estimated coefficients of the simple VAR model for PM2.5 and SO2 regression. The estimated results based on the simple VAR model are summarized in Tables 6 and 7.

The subfigures (I-b) and (II-b) in Figure 6 show the responses of PM2.5 concentration in South Korea to an orthogonalized, one-unit, positive shock of PM2.5 concentration in China in the pre and post COVID-19 periods, respectively. As shown in Figure 6 (I-b), after the PM2.5 shock in China in the pre COVID-19 period, PM2.5 in Korea increased with time lags. The trans-boundary impact of PM2.5 concentration in China reached its peak on the third day[6] and started to decline afterward. On the other hand, by comparing IRFs in Figure 6 (I-b)) and (I-d), we find that the response of PM2.5 concentration in Korea to domestic pollution emissions was larger than its response to trans-boundary PM2.5 pollution from China. This result illustrates that the PM2.5 concentration in Korea is primarily caused by domestic pollution.

In the post COVID-19 period, as displayed in Figure 6 (II-b), an increase in Korea's PM2.5 concentration responses to China could still be observed; compared to the response in Figure 6 (I-b), however, the impact seems to be largely decreased. This result suggests that the lock-down measures adopted following the spread of coronavirus led to an observable decline in the level of trans-boundary PM2.5 pollution transmitted from China to South Korea.

[Figure 6]

The coefficients of L.CPM2.5 and L2.CPM2.5 noted in columns (2) and (4) in Table 6 indicate that the PM2.5 concentration in China is positively and statistically significantly correlated with the PM2.5 concentration in South Korea with a one-day lag time, and negatively correlated with that in South Korea with a two-day lag time. This result illustrates a similar conclusion to the IRFs, which is that the trans-boundary PM2.5 pollution from China is subject to short-term time lags. If we compare the estimated results before and after the spread of COVID-19, we find that

[6] In the figure of IRFs, day 0 is set as the baseline day; thus, the third day represents the day with two-day time lags.

the impact of a one-unit increases in PM2.5 concentration in China on PM2.5 concentration levels in South Korea decreases from 0.049 to 0.001. Simultaneously, the response of PM2.5 concentration in South Korea to domestic pollution emissions has slightly decreased as well, from 0.718 to 0.507.

[Table 6]

As demonstrated in Figure 7 (I-f) one day after China's SO2 concentration increased, the SO2 concentration in Korea started to increase. Similar to the former estimated results, by comparing subfigures (I-f) and (I-h) in Figure 7, we found that SO2 concentration in Korea was mainly caused by domestic pollution. Simultaneously, our results illustrate by (I-f) and (II-f), due to the contraction in economic activity caused by the COVID-19 outbreak, that the transboundary SO2 pollution from China to South Korea has been significantly reduced. On the other hand, according to Figure 7 (I-g), in the pre COVID-19 period, transboundary SO2 pollution from South Korea also exerted a significant impact on pollution levels in China. However, this transboundary SO2 pollution from South Korea could no longer be found in the post COVID-19 period.

[Figure 7]

The coefficients of CSO2 in Table 7 illustrate that the trans-boundary impact of SO2 concentration in China decreased from 0.118 to 0.001 due to the lock-down measures adopted in the post COVID-19 period. On the other hand, owing to the impact of domestic pollution in South Korea on its own, SO2 concentration increased from 0.624 to 0.769. However, trans-boundary SO2 pollution from South Korea was not found to be positively and statistically significantly correlated with pollution in China. These results demonstrate that the SO2 concentration in South Korea was mainly caused by domestic pollution emissions. China was indeed partially responsible for SO2 pollution in South Korea, although it was comparatively smaller than the domestic impact, and the spread of coronavirus further decreased the trans-boundary impact. On the contrary, there was no evidence to support the notion that SO2 emissions in South Korea had similar trans-boundary impacts on pollution in China during the winter and spring seasons.

[Table 7]

### 5.3 Estimation results of VAR-X models

In order to control for climate factors that may also affect the concentration of air pollutants, the VAR-X models used were adapted by adding control variables, including the daily average amount of precipitation, wind speed, and the temperature of capital areas in the simple VAR model.

[Table 8]

As represented by the summarized coefficients of CPM2.5 in column (2) in Table 8, variation in Korea's PM2.5 concentration caused by the one-unit positive shock of PM2.5 concentration in China was positive and significant; this result is in line with the result achieved by the IRFs, which states that Korea's PM2.5 pollution comes partially from China. On the other hand, compared to the pre COVID-19 period, we found that the estimated coefficient of CPM2.5 in the post COVID-19 period decreased from 0.048 to 0.002. This decrease in trans-boundary

PM2.5 pollution may be due to the remarkable improvement in air quality induced by lock-down policies in China. By contrast, the coefficients of KPM2.5 in columns (2) and (4) increased from 0.467 to 0.551 and both were statistically significant at the 1% level. This result indicates the increasing impact of domestic PM2.5 pollution in South Korea in the post COVID-19 period.

[Table 9]

The estimated results of the VAR-X model for the SO2 regression are presented in Table 8. As shown in column (2) in Table 9, the summarized coefficient of CSO2 was 0.016, that of KSO2 was 0.640, and both were statistically significant. These estimated results illustrate that SO2 concentration in China could partly explain the changes in South Korea's air quality in the pre COVID-19 period, while the impact of domestic pollution was nearly 40 times that of trans-boundary pollution. On the other hand, by comparing the estimated coefficients of CSO2 in columns (2) and (4) in Table 9, we found that the trans-boundary SO2 impact of China decreased from 0.016 to 0.006. Our results suggest that the disparity between the impact of trans-boundary pollution and domestic pollution, affected by the COVID-19 outbreak, has been further enlarged.

## 5.4 Estimation results regarding domestic air pollution transmission

Tables 10 and 11 present both trans-boundary and domestic air pollution transmission impacts on PM2.5 and SO2 concentrations in Gyeonggi province, Incheon city, and Seoul city. Our estimated results relayed in columns (1), (3), and (5) based on the pre COVID-19 sample period, the others are estimated results for regression under the post COVID-19 period.

According to the coefficients of IPM2.5 in columns (1) and (5) of Table 10, we found that PM2.5 concentration in Incheon city exerts domestic pollution transmission impact on both Gyeonggi province and Seoul City. On the other hand, in the post COVID-19 period, PM2.5 concentration in Incheon was no longer responsible for PM2.5 pollution level in its surrounding regions. The coefficients of SPM2.5 in columns (2) and (4) of Table 10 are positively and statistically significantly correlated with GPM2.5 and IPM2.5. These estimated coefficients illustrate that, along with the spread of coronavirus, PM2.5 pollutants in Seoul city had displayed that in Incheon city as the main source of PM2.5 concentration in the SCA region.

By comparing the coefficients of CPM2.5 in between pre and post COVID-19 period, we found that the impact of trans-boundary PM2.5 pollution directly from the JJJ region to Gyeonggi province, Incheon city, and Seoul city, had been significantly decreased. For instance, as shown in columns (1) and (2) of Table 10, the impact of trans-boundary PM2.5 pollution directly from the JJJ region to Gyeonggi province decreased from 0.182 to 0.096[7], but remained positive and statistically significant.

On the other hand, as shown by the coefficients of CPM2.5 and IPM2.5 in column (1) of Table 9, compared to the impact of domestic pollution transmission from the Incheon city to Gyeonggi province, trans-boundary PM2.5 pollution transmission from JJJ region in China represented relatively smaller impact on air pollutants in Gyeonggi province. Similarly, domestic PM2.5 pollution's impact in Incheon city was 2.34 times greater than the trans-boundary pollution transmission. Simultaneously, domestic PM2.5 pollution transmission impact from Incheon city to Seoul city was 2.52 times higher than impact of pollutants oriented from JJJ regions in China.

[7] The indirect air pollution transmission from the JJJ region to Gyeonggi province is not considered in this study; thus, the estimated results regarding trans-boundary impact might have been underestimated.

[Table 10]

According to the estimated results regarding the SO2 concentration in Gyeonggi province shown in Table 11, we found that SO2 pollutants in Gyeonggi province remained the main resource of SO2 pollution in SCA region, in both pre and post COVID-19 period. On the other hand, coefficients of ISO2 and SSO2 show statistically insignificant results on GSO2, illustrate that there does not exist domestic SO2 pollution transmission from Incheon and Seoul city to Gyeonggi province. In the post COVID-19 period, direct trans-boundary impact of SO2 concentration in JJJ regions of China, had been significantly decreased as well. For example, the coefficients of CSO2 in columns (1) and (2) indicate that the impact of such trans-boundary pollution on SO2 concentration in Gyeonggi province decreased from 0.074 to 0.021. This result may have been caused by the significant drop in the SO2 concentration level in China, due to the strict lock down measures.

Moreover, by comparing impacts of domestic pollution and trans-boundary pollution transmission, we found that domestic SO2 pollution's impact in Incheon city was 2.27 times greater than the trans-boundary pollution transmission in the pre COVID-19 period. In the post COVID-19 period, this gap between domestic pollution and trans-boundary pollution had been enlarged to 6.33 times.

[Table 11]

## 5.5 Robustness check

As a robustness check for the main regression estimated by the two-period model, an estimation based on the VAR-X model with a sample period spanning from January 1, 2019, to December 31, 2019, was adopted to indicate trans-boundary air pollution between China and South Korea without controlling for seasonal impacts. We limited the sample period to the first half of 2019 and 2020 for the main regression because we assumed that dust storms mainly occur during the winter and spring seasons. Therefore, the year-long sample period was able to help us investigate the overall impact of transboundary air pollution without considering wind directions.

As shown in column (4) of Table A1, during the entire course of 2019, a 0.064 unit increase in PM2.5 concentration in China was able to cause a one-unit increase in PM2.5 concentration in South Korea. Comparatively, this one-unit increase in South Korea was caused by a 0.691 unit increase in its own PM2.5 emissions on the last day. This result illustrates that the domestic impact on PM2.5 concentration in South Korea is about 10.8 times greater than the trans-boundary impact exerted by China. Similarly, the coefficients of L.CSO2 and L2.CSO2 in column (4) of Table A2 indicate that a one-unit positive shock of SO2 concentration in China was able to cause a 0.031 unit positive variation in South Korea's SO2 concentration. On the other hand, a 0.678 unit increase in SO2 emissions in South Korea was able to cause by a one-unit shock of domestic pollution.

These results confirmed our conclusions from the main regression, which were that China's air pollutants did indeed transmit pollution across the national boundary, while domestic pollutants were still the main sources of air pollution in South Korea.

Additionally, the coefficients of L.KSO2 and L2.KSO2 in column (2) of Table A2 illustrate that a one-unit increase in South Korea's SO2 concentration was able to cause a 0.091 unit positive variation in SO2 concentration in China. Subfigure (IV-g) of Figure A2 shows that South Korea's SO2 concentration exerted a positive and significant impact on that of China, and this impact lasted for two days. This estimated result, over the year-long sample, illustrates that trans-boundary SO2 pollution occurred both directions; the trans-boundary impact of SO2 concentration did not only exist across the “China to South Korea" route, but also in the opposite direction.

## 6 Conclusions

The estimated results of this study concluded that Korea's $PM_{2.5}$ and $SO_2$ concentrations are indeed partly affected by China, while domestic pollution is still the main source of air pollution in Korea. This result is aligned with the joint research conducted by NASA and South Korea’s National Institute of Environmental Research, which claims that over half of the air pollution in South Korea derives from local causes material[8]. We found that main source of domestic pollution transmission in South Korea contains strong regional characteristics. Conclusions drawn by estimated results indicate that $SO_2$ pollutants in capital regions of South Korea mainly orient from Gyeonggi province, a region developed in heavy industry. On the other hand, $PM_{2.5}$ emissions in Incheon and Seoul city, regions with heavy population density and vehicle use, have greater responsibility in domestic pollution transmission. To prevent such high concentrations and pollution transmission among regions, domestic measures to reduce air pollutants are urgently needed.

Moreover, based on the estimated results, this study indicates that, during the COVID- 19 outbreak, lock-down measures led to a decrease in the trans-boundary impact of both PM2.5 and SO2 concentration from China to South Korea. An enlarged gap between effect of domestic pollutions and trans-boundary pollutions has been noted. The findings of this study can be taken to inform policy design for multiple countries: forceful environmental protection efforts at the domestic level may lead to an improvement in the environmental conditions of nearby countries as well.

However, as an unprecedented measure in an effort to quarantine the outbreak of COVID-19, we consider the impact of lock-down on reducing the trans-boundary air pollution is temporary. Being the first country to be hit by the COVID-19 outbreak, China is also among the first economies that are recovering rapidly from the outbreak. The rebound of emissions from power plants, industry and transport were observed, as the lock-down measures were lifted, economic activity and industrial production was resumed in the country. In October 2020, $PM_{2.5}$ concentrations in the JJJ region, was observed an increase of 15.6% over the monthly levels recorded in the previous year (Huang, 2021). The government should further strengthen efforts towards emission mitigation, in order to reduce the harmful effects of trans-boundary air pollution on residents of other countries.

Furthermore, understanding of trans-boundary transports of air pollutants will advance the predictability of local air quality, and will encourage the development of international measures to improve air quality (Oh et al, 2015). Our estimation results conclude that trans- boundary air pollution did not only exist across the “China to South Korea” route, but also in the “South Korea to China” direction. Because of the trans-boundary nature of air pollution, international treaties should be ratified by the neighboring countries. For instance, the effort to combat thinning of the ozone layer, is regulated by the Vienna Convention of 1985 and subsequent protocols (Ministry of the Environment of Denmark, n.d.). Similarly, in order to address the acid rain and trans-boundary air pollution issue, Canada and the US made commitments under the 1991 Air Quality Agreement. As result, Canada and the US have not only successfully reduced emissions of $SO_2$ and $NO_x$ - the major contributors of acid rain- but also surpassed reduction requirements of the Agreement (Air Quality Agreement, 2000). We suggest that

[8] Retrieved April 8, 2021, from
<http://english.hani.co.kr/arti/english_edition/e_international/803654.html>

similar international conventions and cooperative efforts should be adopted to reduce trans-boundary pollution in the East Asian countries as well.

Table 1. Summary Statistics

| | | pre COVID-19 | | | post COVID-19 | | |
|---|---|---|---|---|---|---|---|
| Variables | Unit | Obs | Mean | Std.Dev. | Obs | Mean | Std.Dev. |
| **China (C): JJJ region** | | | | | | | |
| *Pollution indicator* | | | | | | | |
| CPM2.5 | $\mu g/m^3$ | 155 | 124.6 | 51.58 | 156 | 117.4 | 51.45 |
| $CSO_2$ | $\mu g/m^3$ | 155 | 21.65 | 11.74 | 156 | 13.66 | 6.129 |
| *Control variables* | | | | | | | |
| Precipitation_c | mm | 155 | 0.510 | 2.238 | 156 | 0.728 | 2.605 |
| Wind Speed_c | km/h | 155 | 9.802 | 2.841 | 156 | 9.321 | 3.175 |
| Temperature_c | °C | 155 | 9.978 | 9.622 | 156 | 10.32 | 8.862 |
| **South Korea (K): SCA region** | | | | | | | |
| *Pollution indicator* | | | | | | | |
| KPM2.5 | $\mu g/m^3$ | 155 | 99.03 | 32.12 | 156 | 79.96 | 26.15 |
| $KSO_2$ | $\mu g/m^3$ | 155 | 23.23 | 5.956 | 156 | 13.44 | 3.671 |
| *Control variables* | | | | | | | |
| Precipitation_k | mm | 155 | 0.865 | 3.307 | 156 | 1.589 | 5.129 |
| Wind Speed_k | km/h | 155 | 12.76 | 3.940 | 156 | 15.58 | 5.694 |
| Temperature_k | °C | 155 | 8.158 | 7.869 | 156 | 8.554 | 6.879 |

Table 2. Summary Statistics

| | | pre COVID-19 | | | post COVID-19 | | |
|---|---|---|---|---|---|---|---|
| Variables | Unit | Obs | Mean | Std.Dev. | Obs | Mean | Std.Dev. |
| **China (C): JJJ region** | | | | | | | |
| *Pollution indicator* | | | | | | | |
| CPM2.5 | $\mu g/m^3$ | 155 | 124.6 | 51.58 | 156 | 117.4 | 51.45 |
| $CSO_2$ | $\mu g/m^3$ | 155 | 21.65 | 11.74 | 156 | 13.66 | 6.129 |
| *Control variables* | | | | | | | |
| Precipitation_c | mm | 155 | 0.510 | 2.238 | 156 | 0.728 | 2.605 |
| Wind Speed_c | km/h | 155 | 9.802 | 2.841 | 156 | 9.321 | 3.175 |
| Temperature_c | °C | 155 | 9.978 | 9.622 | 156 | 10.32 | 8.862 |
| **South Korea (G): Gyeonggi province** | | | | | | | |
| *Pollution indicator* | | | | | | | |
| GPM2.5 | $\mu g/m^3$ | 155 | 89.72 | 35.62 | 156 | 73.92 | 28.61 |
| $GSO_2$ | $\mu g/m^3$ | 155 | 15.39 | 3.209 | 156 | 8.994 | 2.110 |
| *Control variables* | | | | | | | |
| Precipitation_g | mm | 155 | 0.813 | 3.154 | 156 | 1.952 | 7.361 |
| Wind Speed_g | km/h | 155 | 7.510 | 3.270 | 156 | 8.404 | 4.073 |
| Temperature_g | °C | 155 | 6.155 | 8.400 | 156 | 7.141 | 7.303 |
| **South Korea (I): Incheon city** | | | | | | | |
| *Pollution indicator* | | | | | | | |
| IPM2.5 | $\mu g/m^3$ | 155 | 82.01 | 32.18 | 156 | 64.77 | 23.91 |
| $ISO_2$ | $\mu g/m^3$ | 155 | 20.13 | 4.842 | 156 | 13.98 | 3.196 |
| *Controlvariables* | | | | | | | |
| Precipitation_i | mm | 155 | 0.866 | 3.307 | 156 | 1.589 | 5.129 |
| WindSpeed_i | km/h | 155 | 12.76 | 3.940 | 156 | 15.58 | 5.694 |
| Temperature_i | °C | 155 | 8.158 | 7.869 | 156 | 8.554 | 6.879 |
| **South Korea (S): Seoul city** | | | | | | | |
| *Pollution indicator* | | | | | | | |
| SPM2.5 | $\mu g/m^3$ | 155 | 88.49 | 34.01 | 156 | 75.00 | 26.83 |
| $SSO_2$ | $\mu g/m^3$ | 155 | 17.87 | 3.385 | 156 | 11.45 | 3.308 |
| *Controlvariables* | | | | | | | |
| Precipitation_s | mm | 155 | 0.866 | 3.307 | 156 | 1.589 | 5.129 |
| WindSpeed_s | km/h | 155 | 12.76 | 3.940 | 156 | 15.58 | 5.694 |
| Temperature_s | °C | 155 | 8.158 | 7.869 | 156 | 8.554 | 6.879 |

Table 3. Unit root tests

| | ADF | | PP | | KPSS | |
|---|---|---|---|---|---|---|
| | No trend | With trend | No trend | With trend | No trend | With trend |
| $CPM_{2.5}$ | -11.239*** | -11.305*** | -10.543*** | -10.600*** | 0.874 | 0.825 |
| CSO2 | -9.292*** | -10.069*** | -9.685*** | -10.582*** | 5.050 | 1.880 |
| $KPM_{2.5}$ | -10.288*** | -10.777*** | -8.582*** | -8.906*** | 2.790 | 1.340 |
| KSO2 | -7.004*** | -9.547*** | -7.305*** | -9.821*** | 11.20 | 1.100 |
| precipitation_c | -14.154*** | -14.144*** | -18.175*** | -18.161*** | 0.575* | 0.546 |
| ws_c | -10.805*** | -10.795*** | -13.662*** | -13.648*** | 1.460 | 1.470 |
| temperature_c | -2.393* | -2.391* | -2.393* | -2.390* | 3.410 | 3.450 |
| precipitation_k | -14.040*** | -14.028*** | -17.136*** | -17.122*** | 0.467 | 0.472 |
| ws_k | -11.666*** | -12.491*** | -14.300*** | -15.117*** | 3.590 | 0.623 |
| temperature_k | -3.063** | -3.061** | -3.064** | -3.060* | 3.790 | 3.820 |

Note: ADF refers to Augmented Dickey-Fuller test, PP refers to Phillips Perron test, KPSS refers to Kwiatkowski-Phillips-Schmidt-Shin test; *, **, *** indicate rejection of the null hypothesis at 10%, 5%, and 1%, respectively.

Table 4. Lag order selection statistics for simple VAR model

| lag | LR | FPE | AIC | HQIC | SBIC |
|---|---|---|---|---|---|
| Panel A. PM2.5 | | | | | |
| 0 | | 1700000 | 19.9978 | 20.0143 | 20.0385 |
| 1 | 217.2 | 399876 | 18.5747 | 18.6242 | 18.6967 |
| 2 | 31.286 | 341309 | 18.4162 | 18.4989* | 18.6197* |
| 3 | **12.763*** | **330458*** | **18.3838*** | 18.4996 | 18.6686 |
| 4 | 0.49042 | 347835 | 18.4349 | 18.5837 | 18.8011 |
| 5 | 9.3533 | 344735 | 18.4257 | 18.6076 | 18.8733 |
| 6 | 8.7322 | 343148 | 18.4207 | 18.6356 | 18.9497 |
| | | | | | |
| Panel B. $SO_2$ | | | | | |
| 0 | | 273.371 | 11.2866 | 11.303 | 11.3271 |
| 1 | 192.34 | 78.671 | 10.041 | 10.0904* | 10.1625* |
| 2 | **10.225*** | **77.500*** | **10.026*** | 10.1083 | 10.2285 |
| 3 | 6.8284 | 78.1231 | 10.0339 | 10.1491 | 10.3174 |
| 4 | 8.5108 | 77.8663 | 10.0304 | 10.1786 | 10.395 |
| 5 | 1.5066 | 81.3789 | 10.0743 | 10.2553 | 10.5199 |
| 6 | 4.2451 | 83.4999 | 10.0997 | 10.3136 | 10.6262 |

Note:* indicates optimal lag order selection according to each statistic.

Table 5. Granger causality test results

Panel A. PM2.5

| Null hypothesis | Obs | F-Statistic | P-value | Conclusion |
|---|---|---|---|---|
| **pre COVID-19** | | | | |
| CPM2.5 cannot Granger cause KPM2.5 | 152 | 10.67 | 0.0000 | Reject null hypothesis |
| KPM2.5 cannot Granger cause CPM2.5 | 152 | 0.270 | 0.8475 | Accept null hypothesis |
| **post COVID-19** | | | | |
| CPM2.5 cannot Granger cause KPM2.5 | 153 | 10.11 | 0.0000 | Reject null hypothesis |
| KPM2.5 cannot Granger cause CPM2.5 | 153 | 1.440 | 0.2335 | Accept null hypothesis |

Panel B. $SO_2$

| Null hypothesis | Obs | F-Statistic | P-value | Conclusion |
|---|---|---|---|---|
| **pre COVID-19** | | | | |
| $CSO_2$ cannot Granger cause $KSO_2$ | 153 | 3.470 | 0.0335 | Accept null hypothesis |
| $KSO_2$ cannot Granger cause $CSO_2$ | 153 | 5.450 | 0.0052 | Reject null hypothesis |
| **post COVID-19** | | | | |
| $CSO_2$ cannot Granger cause $KSO_2$ | 154 | 4.300 | 0.0152 | Accept null hypothesis |
| $KSO_2$ cannot Granger cause $CSO_2$ | 154 | 1.300 | 0.2757 | Accept null hypothesis |

Note: pre COVID-19 is period between 1 January 2019 and 4 June 2019, and that of post COVID-19 is the same period in 2020. The conclusions in this table are judged at significance level of 1%.

Table 6. Simple VAR-X estimation results on PM2.5 concentration

| | pre COVID-19 | | post COVID-19 | |
|---|---|---|---|---|
| | CPM2.5 | KPM2.5 | CPM2.5 | KPM2.5 |
| | (1) | (2) | (3) | (4) |
| L.CPM2.5 | 0.716*** | **0.209***** | 0.922*** | **0.183***** |
| | (0.092) | (0.037) | (0.081) | (0.033) |
| L2.CPM2.5 | -0.187* | **-0.160***** | -0.388*** | **-0.182***** |
| | (0.110) | (0.045) | (0.109) | (0.045) |
| L3.CPM2.5 | 0.020 | 0.0512 | 0.139 | 0.066* |
| | (0.100) | (0.041) | (0.087) | (0.036) |
| L.KPM2.5 | 0.175 | **1.035***** | 0.167 | **1.086***** |
| | (0.218) | (0.089) | (0.197) | (0.080) |
| L2.KPM2.5 | -0.14 | **-0.521***** | -0.400 | **-0.579***** |
| | (0.277) | (0.113) | (0.255) | (0.104) |
| L3.KPM2.5 | 0.085 | **0.204***** | 0.374** | 0.108 |
| | (0.180) | (0.074) | (0.177) | (0.072) |
| cons | 43.64*** | 15.52*** | 26.47** | 22.51*** |
| | (11.81) | (4.814) | (11.69) | (4.775) |
| R-squared | 0.445 | 0.768 | 0.560 | 0.702 |
| S.E.equation | 39.03 | 15.92 | 34.95 | 14.27 |
| F-statistic | 20.32 | 84.05 | 32.43 | 59.99 |
| AIC | 18.36 | | 18.17 | |

Note: standard errors in parentheses, * $p < 0.1$, ** $p < 0.05$, *** $p < 0.01$

Table 7. Simple VAR-X estimation results on SO2 concentration

| | pre COVID-19 | | post COVID-19 | |
|---|---|---|---|---|
| | $CSO_2$ | $KSO_2$ | $CSO_2$ | $KSO_2$ |
| | (1) | (2) | (3) | (4) |
| L.$CSO_2$ | 0.552*** | **0.118***** | 0.623*** | **0.094***** |
| | (0.080) | (0.044) | (0.076) | (0.036) |
| L2.$CSO_2$ | 0.094 | -0.073 | -0.211*** | **-0.093**** |
| | (0.079) | (0.044) | (0.076) | (0.036) |
| L.$KSO_2$ | 0.400*** | **0.624***** | 0.112 | **0.916***** |
| | (0.149) | (0.083) | (0.172) | (0.081) |
| L2.$KSO_2$ | -0.466*** | -0.093 | 0.079 | **-0.147*** |
| | (0.148) | (0.082) | (0.168) | (0.079) |
| cons | 8.841*** | 9.869*** | 5.224*** | 3.015*** |
| | (2.978) | (1.653) | (1.393) | (0.655) |
| R-squared | 0.458 | 0.413 | 0.389 | 0.688 |
| S.E.equation | 8.374 | 4.646 | 4.329 | 2.035 |
| F-statistic | 32.38 | 26.87 | 24.52 | 84.97 |
| AIC | 12.98 | | 10.02 | |

Note: standard errors in parentheses, * $p < 0.1$, ** $p < 0.05$, *** $p < 0.01$

Table 8. VAR-X estimation results on $PM_{2.5}$ concentration

| | pre COVID-19 | | post COVID-19 | |
|---|---|---|---|---|
| | CPM2.5 | KPM2.5 | CPM2.5 | KPM2.5 |
| | (1) | (2) | (3) | (4) |
| L.CPM2.5 | 0.699*** | **0.199***** | 0.783*** | **0.141***** |
| | (0.082) | (0.043) | (0.074) | (0.034) |
| L2.CPM2.5 | -0.149 | **-0.151***** | -0.348*** | **-0.139***** |
| | (0.097) | (0.045) | (0.096) | (0.045) |
| L3.CPM2.5 | -0.030 | 0.044 | 0.059 | 0.054 |
| | (0.090) | (0.041) | (0.079) | (0.035) |
| L.KPM2.5 | 0.085 | **1.003***** | 0.161 | **0.981***** |
| | (0.194) | (0.089) | (0.178) | (0.085) |
| L2.KPM2.5 | 0.023 | **-0.491***** | -0.325 | **-0.515***** |
| | (0.247) | (0.111) | (0.227) | (0.103) |
| L3.KPM2.5 | -0.001 | 0.189*** | 0.205 | 0.054 |
| | (0.160) | (0.072) | (0.162) | (0.072) |
| precipitation_c | -0.799 | | 0.595 | |
| | (1.243) | | (0.963) | |
| ws_c | -6.601*** | | -5.065*** | |
| | (1.054) | | (0.895) | |
| temperature_c | 0.198 | | -0.563 | |
| | (0.347) | | (0.378) | |
| precipitation_k | | -0.924** | | 0.025 |
| | | (0.380) | | (0.238) |
| ws_k | | -0.048 | | -0.431* |
| | | (0.416) | | (0.242) |
| temperature_k | | -0.199 | | -0.651*** |
| | | (0.175) | | (0.194) |
| cons | 112.1*** | 21.28** | 108.7*** | 43.71*** |
| | (15.51) | (9.893) | (16.85) | (7.943) |
| R-squared | 0.569 | 0.780 | 0.596 | 0.725 |
| S.E.equation | 34.75 | 15.67 | 33.84 | 13.86 |
| F-statistic | 22.33 | 59.91 | 25.06 | 44.71 |
| AIC | 18.12 | 18.34 | 17.97 | 18.10 |

Note: standard errors in parentheses, * $p < 0.1$, ** $p < 0.05$, *** $p < 0.01$

Table 9. VAR-X estimation results on $SO_2$ concentration

| | pre COVID-19 | | post COVID-19 | |
|---|---|---|---|---|
| | $CSO_2$ | $KSO_2$ | $CSO_2$ | $KSO_2$ |
| | (1) | (2) | (3) | (4) |
| L.$CSO_2$ | 0.433*** | **0.114**** | 0.489*** | **0.072**** |
| | (0.081) | (0.048) | (0.074) | (0.034) |
| L2.$CSO_2$ | 0.032 | **-0.098**** | -0.150** | **-0.066*** |
| | (0.078) | (0.048) | (0.071) | (0.034) |
| L.$KSO_2$ | 0.324** | **0.640***** | 0.113 | **0.785***** |
| | (0.148) | (0.083) | (0.161) | (0.081) |
| L2.$KSO_2$ | -0.349** | -0.101 | -0.066 | **-0.157**** |
| | (0.142) | (0.090) | (0.157) | (0.075) |
| precipitation_c | -0.546* | | -0.492*** | |
| | (0.288) | | (0.124) | |
| wind speed_c | -0.487* | | -0.478*** | |
| | (0.271) | | (0.120) | |
| temperature_c | -0.245*** | | -0.005 | |
| | (0.079) | | (0.048) | |
| precipitation_k | | 0.103 | | 0.030 |
| | | (0.117) | | (0.032) |
| wind speed_k | | -0.108 | | 0.048 |
| | | (0.114) | | (0.032) |
| temperature_k | | -0.062 | | -0.127*** |
| | | (0.059) | | (0.032) |
| cons | 19.37*** | 12.13*** | 13.04*** | 5.150*** |
| | (4.437) | (2.975) | (2.282) | (1.312) |
| R-squared | 0.528 | 0.422 | 0.495 | 0.737 |
| S.E.equation | 7.897 | 4.655 | 3.976 | 1.889 |
| F-statistic | 24.46 | 15.97 | 21.58 | 61.58 |
| AIC | 12.84 | 12.95 | 9.797 | 9.875 |

Note: standard errors in parentheses, * $p < 0.1$, ** $p < 0.05$, *** $p < 0.01$

Table 10. VAR-X estimation results on $PM_{2.5}$ concentration

*Sample area: Gyeonggi province, Incheon city, Seoul city, JJJ region*

| | GPM2.5 | | IPM2.5 | | SPM2.5 | |
|---|---|---|---|---|---|---|
| | pre COVID-19 | post COVID-19 | pre COVID-19 | post COVID-19 | pre COVID-19 | post COVID-19 |
| | (1) | (2) | (3) | (4) | (5) | (6) |
| L.GPM2.5 | 0.303 | -0.010 | 0.303 | -0.154 | 0.334 | -0.354 |
| | (0.343) | (0.323) | (0.343) | (0.292) | (0.358) | (0.317) |
| L2.GPM2.5 | -0.074 | -0.209 | -0.074 | -0.423 | -0.097 | -0.357 |
| | (0.326) | (0.316) | (0.326) | (0.288) | (0.340) | (0.312) |
| L.IPM2.5 | **0.635*** ** | 0.055 | **0.635*** ** | 0.281 | **0.429* ** | 0.190 |
| | (0.227) | (0.237) | (0.227) | (0.219) | (0.236) | (0.238) |
| L2.IPM2.5 | -0.280 | 0.218 | -0.28 0 | **0.369* ** | -0.360 | 0.354 |
| | (0.221) | (0.236) | (0.221) | (0.213) | (0.230) | (0.231) |
| L.SPM2.5 | -0.349 | **0.734** ** | -0.349 | **0.466* ** | -0.110 | **0.897*** ** |
| | (0.348) | (0.308) | (0.348) | (0.274) | (0.362) | (0.297) |
| L2.SPM2.5 | 0.266 | -0.231 | 0.266 | -0.081 | 0.301 | -0.203 |
| | (0.315) | (0.311) | (0.315) | (0.281) | (0.329) | (0.305) |
| L.CPM2.5 | **0.271*** ** | **0.187*** ** | **0.271*** ** | **0.100** ** | **0.271*** ** | **0.128*** ** |
| | (0.051) | (0.040) | (0.051) | (0.038) | (0.053) | (0.041) |
| L2.CPM2.5 | **-0.089* ** | **-0.091** ** | **-0.089* ** | -0.007 | **-0.101** ** | -0.049 |
| | (0.048) | (0.042) | (0.048) | (0.039) | (0.050) | (0.042) |
| $\text{precipitation}_g$ | -1.520*** | -0.129 | | | | |
| | (0.466) | (0.201) | | | | |
| $\text{ws}_g$ | -0.516 | -1.597*** | | | | |
| | (0.528) | (0.386) | | | | |
| $\text{temperature}_g$ | 0.198 | -0.522** | | | | |
| | (0.368) | (0.226) | | | | |
| $\text{precipitation}_i$ | | | -1.520*** | -0.172 | | |
| | | | (0.466) | (0.269) | | |
| $\text{ws}_i$ | | | -0.516 | -1.000*** | | |
| | | | (0.528) | (0.267) | | |
| $\text{temperature}_i$ | | | 0.198 | -0.788*** | | |
| | | | (0.368) | (0.231) | | |
| $\text{precipitation}_s$ | | | | | -1.745*** | -0.381 |
| | | | | | (0.486) | (0.292) |
| $\text{ws}_s$ | | | | | -0.642 | -0.932*** |
| | | | | | (0.550) | (0.289) |
| $\text{temperature}_s$ | | | | | 0.089 | -0.842*** |
| | | | | | (0.383) | (0.251) |
| cons | 23.49** | 40.54*** | 23.49** | 48.06*** | 32.39*** | 53.23*** |
| | (11.76) | (6.729) | (11.76) | (7.879) | (12.25) | (8.551) |
| R-squared | 0.726 | 0.655 | 0.680 | 0.602 | 0.681 | 0.627 |
| S.E.equation | 19.61 | 17.36 | 19.18 | 15.65 | 19.99 | 16.99 |
| F-statistic | 36.10 | 26.62 | 28.98 | 21.17 | 29.12 | 23.58 |
| AIC | 31.59 | 30.81 | 31.80 | 30.77 | 31.80 | 30.77 |

Note: standard errors in parentheses, * $p < 0.1$, ** $p < 0.05$, *** $p < 0.01$

Table 11. VAR-X estimation results on $SO_2$ concentration

*Sample area: Gyeonggi province, Incheon city, Seoul city, JJJ region*

| | $GSO_2$ | | $ISO_2$ | | $SSO_2$ | |
|---|---|---|---|---|---|---|
| | pre COVID-19 | post COVID-19 | pre COVID-19 | post COVID-19 | pre COVID-19 | post COVID-19 |
| | (1) | (2) | (3) | (4) | (5) | (6) |
| $L.GSO_2$ | **0.422*** | **0.151*** | **0.364*** | -0.020 | **0.303*** | **0.323*** |
| | (0.114) | (0.109) | (0.178) | (0.147) | (0.112) | (0.164) |
| $L2.GSO_2$ | 0.075 | -0.002 | -0.178 | -0.329** | -0.101 | -0.227 |
| | (0.114) | (0.108) | (0.175) | (0.150) | (0.111) | (0.167) |
| $L.ISO_2$ | -0.131 | 0.133 | **0.354*** | **0.401*** | 0.042 | 0.191 |
| | (0.083) | (0.088) | (0.131) | (0.118) | (0.083) | (0.132) |
| $L2.ISO_2$ | -0.079 | 0.004 | -0.095 | **0.213*** | -0.121 | 0.052 |
| | (0.081) | (0.082) | (0.127) | (0.110) | (0.081) | (0.123) |
| $L.SSO_2$ | 0.0391 | 0.009 | 0.023 | 0.124 | **0.218*** | 0.037 |
| | (0.114) | (0.052) | (0.178) | (0.071) | (0.112) | (0.080) |
| $L2.SSO_2$ | 0.107 | 0.038 | 0.229 | -0.025 | **0.268*** | 0.0868 |
| | (0.115) | (0.053) | (0.176) | (0.071) | (0.111) | (0.079) |
| $L.CSO_2$ | **0.121*** | **0.067*** | **0.156*** | **0.097*** | **0.112*** | **0.106*** |
| | (0.026) | (0.025) | (0.039) | (0.034) | (0.025) | (0.038) |
| $L2.CSO_2$ | **-0.047*** | **-0.046*** | -0.048 | -0.026 | -0.043 | -0.009 |
| | (0.026) | (0.026) | (0.042) | (0.034) | (0.027) | (0.039) |
| $precipitation_g$ | -0.199*** | -0.036** | | | | |
| | (0.064) | (0.017) | | | | |
| $ws_g$ | -0.070 | -0.076** | | | | |
| | (0.072) | (0.034) | | | | |
| $temperature_g$ | 0.048 | -0.080*** | | | | |
| | (0.033) | (0.021) | | | | |
| $precipitation_i$ | | | 0.046 | 0.006 | | |
| | | | (0.097) | (0.034) | | |
| $ws_i$ | | | 0.173* | 0.010 | | |
| | | | (0.094) | (0.034) | | |
| $temperature_i$ | | | 0.099* | -0.143*** | | |
| | | | (0.056) | (0.032) | | |
| $precipitation_s$ | | | | | 0.257*** | 0.260*** |
| | | | | | (0.061) | (0.038) |
| $ws_s$ | | | | | 0.025 | 0.013 |
| | | | | | (0.059) | (0.038) |
| $temperature_s$ | | | | | -0.035 | -0.165*** |
| | | | | | (0.035) | (0.036) |
| cons | 8.158*** | 6.169*** | 2.211 | 7.445*** | 5.925*** | 5.247*** |
| | (1.710) | (0.957) | (2.918) | (1.509) | (1.845) | (1.686) |
| R-squared | 0.468 | 0.553 | 0.446 | 0.651 | 0.547 | 0.601 |
| S.E.equation | 2.450 | 1.443 | 3.783 | 1.936 | 2.391 | 2.163 |
| F-statistic | 12.00 | 17.29 | 10.96 | 26.10 | 16.46 | 21.11 |
| AIC | 20.64 | 17.39 | 20.53 | 17.18 | 20.53 | 17.18 |

Note: standard errors in parentheses, * $p < 0.1$, ** $p < 0.05$, *** $p < 0.01$

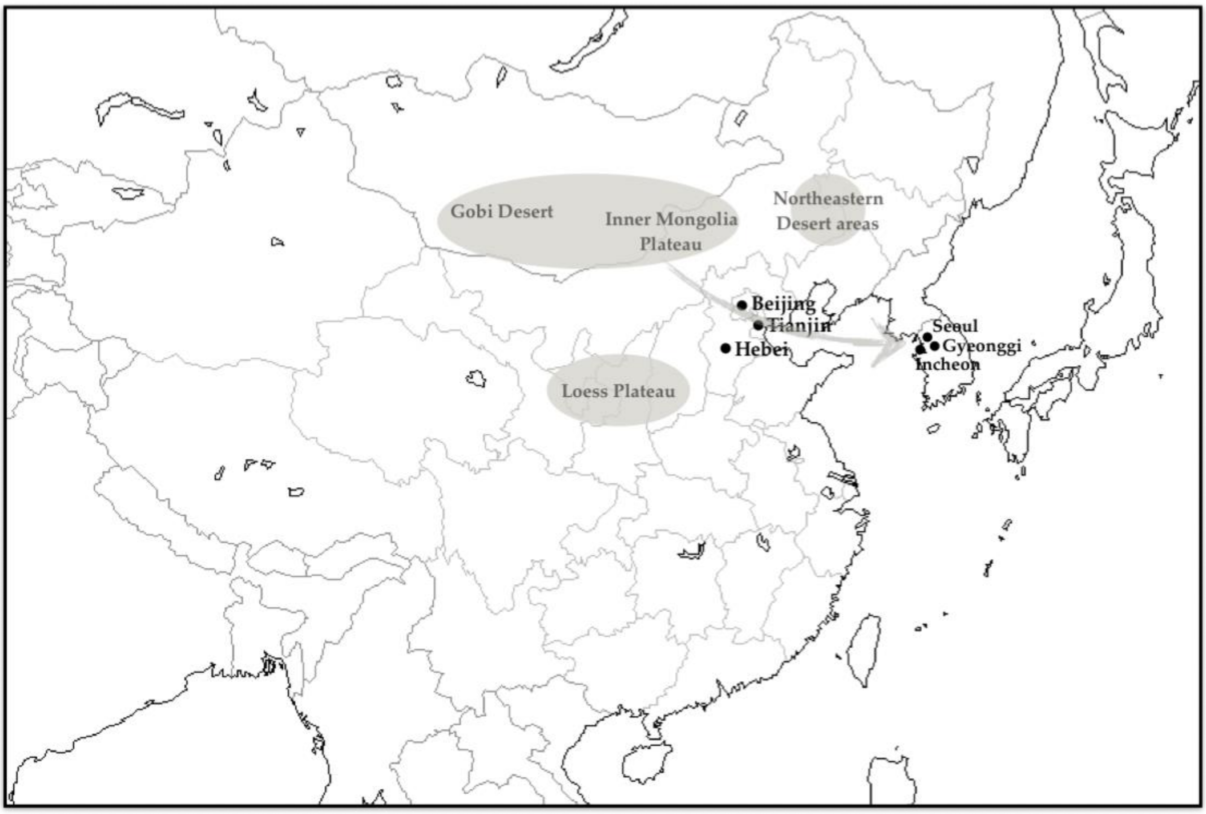


Figure 1. The source of yellow dust in South Korea. Arrow mark shows the rough route of dust storm come directly from the Gobi Desert and the Inner Mongolian plateau.

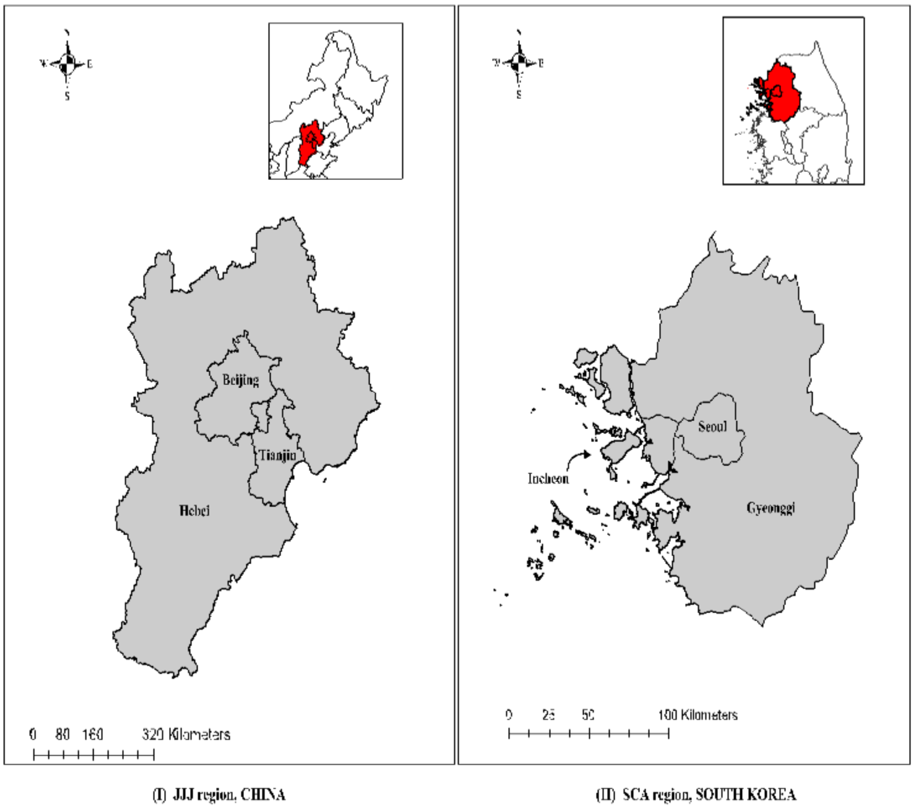


Figure 2. Locations of capital areas in China and South Korea.

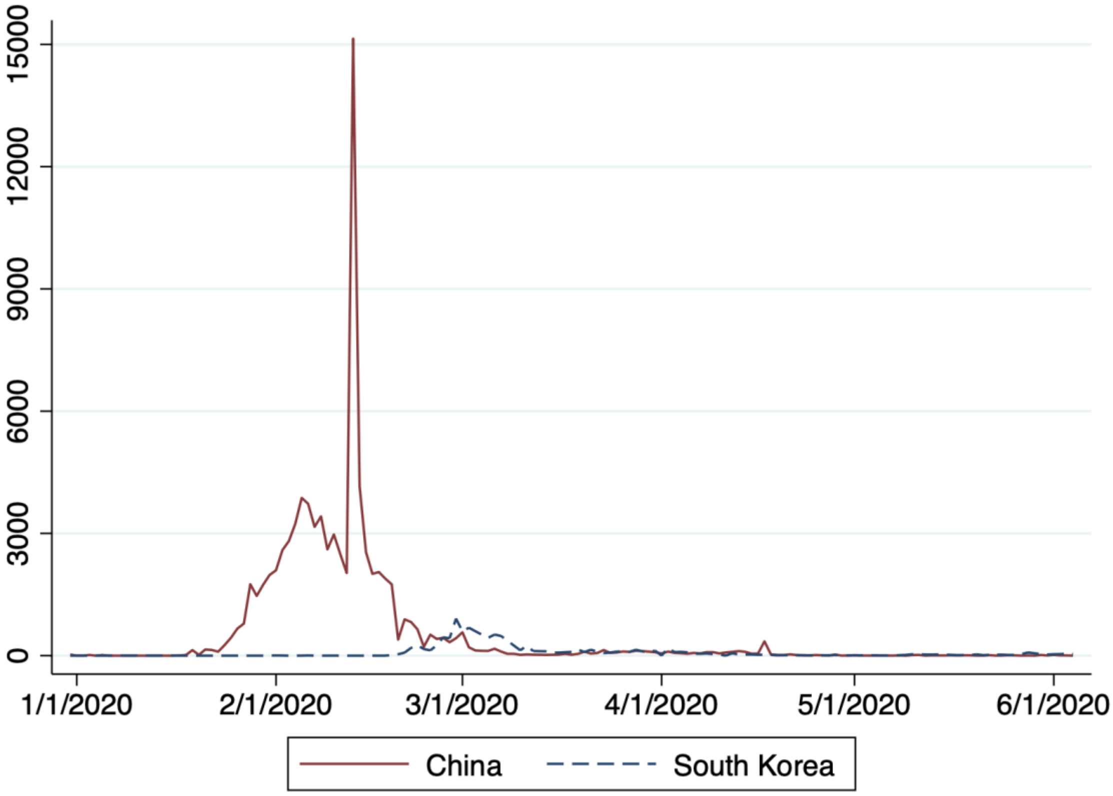


Figure 3. Trends in daily confirmed cases of the COVID-19 in China and South Korea

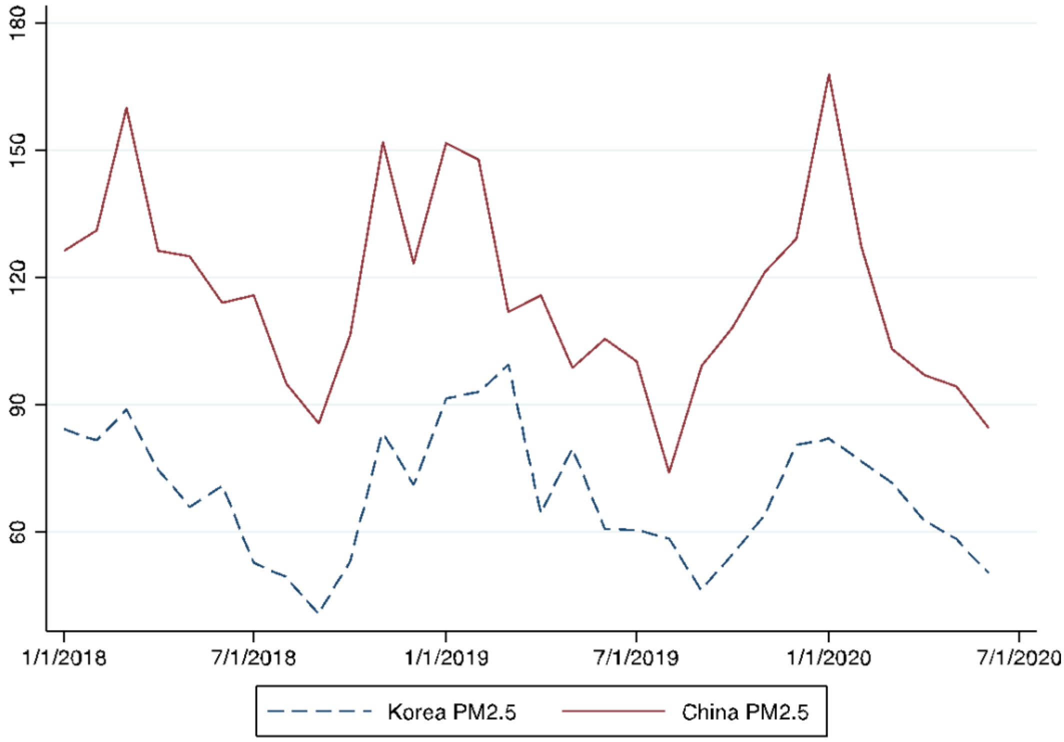


Figure 4. Trends in monthly $PM_{2.5}$ concentration in capital area of China and South Korea ($\mu g/m^3$, 2018-2020)

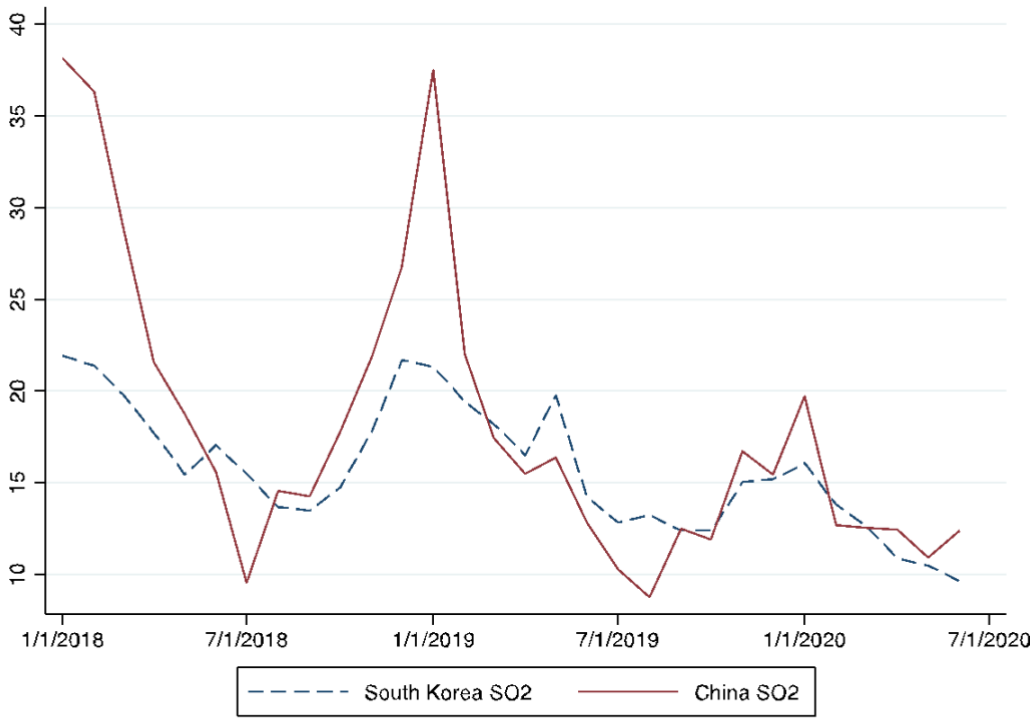


Figure 5. Trends in monthly $SO_2$ concentration in capital area of China and South Korea ($\mu g/m^3$, 2018-2020)

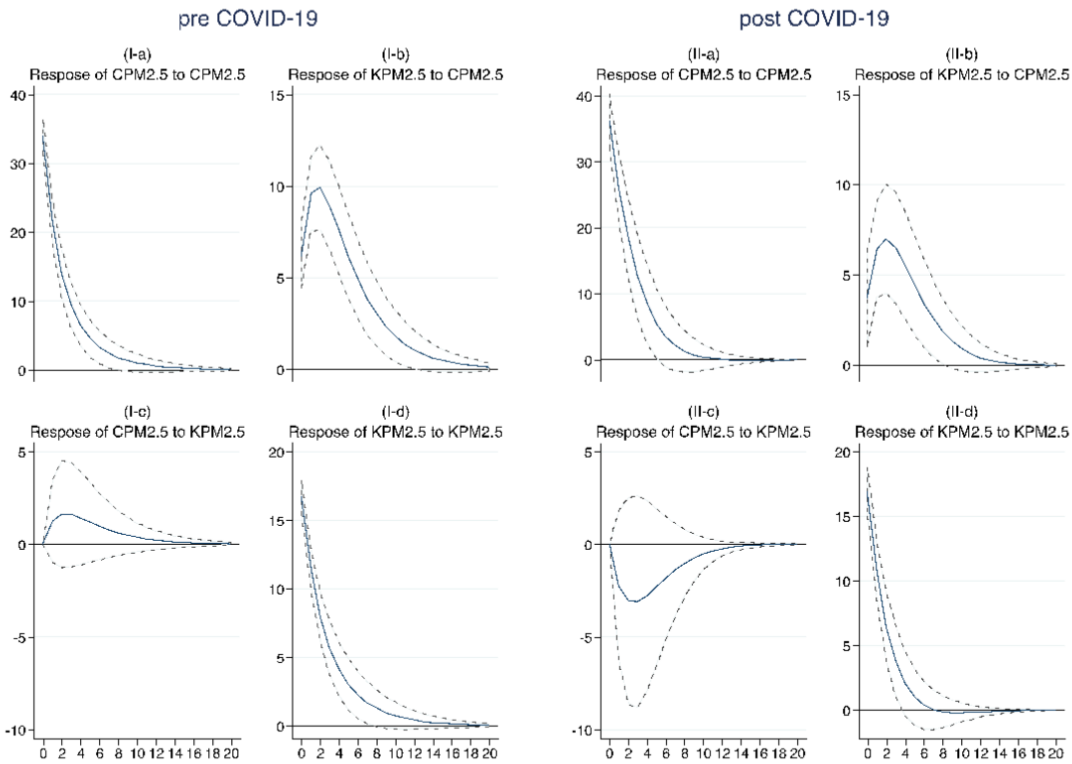


Figure 6. Impulse response of $PM_{2.5}$ concentration (μg/m$^3$)
in capital areas of China and South Korea

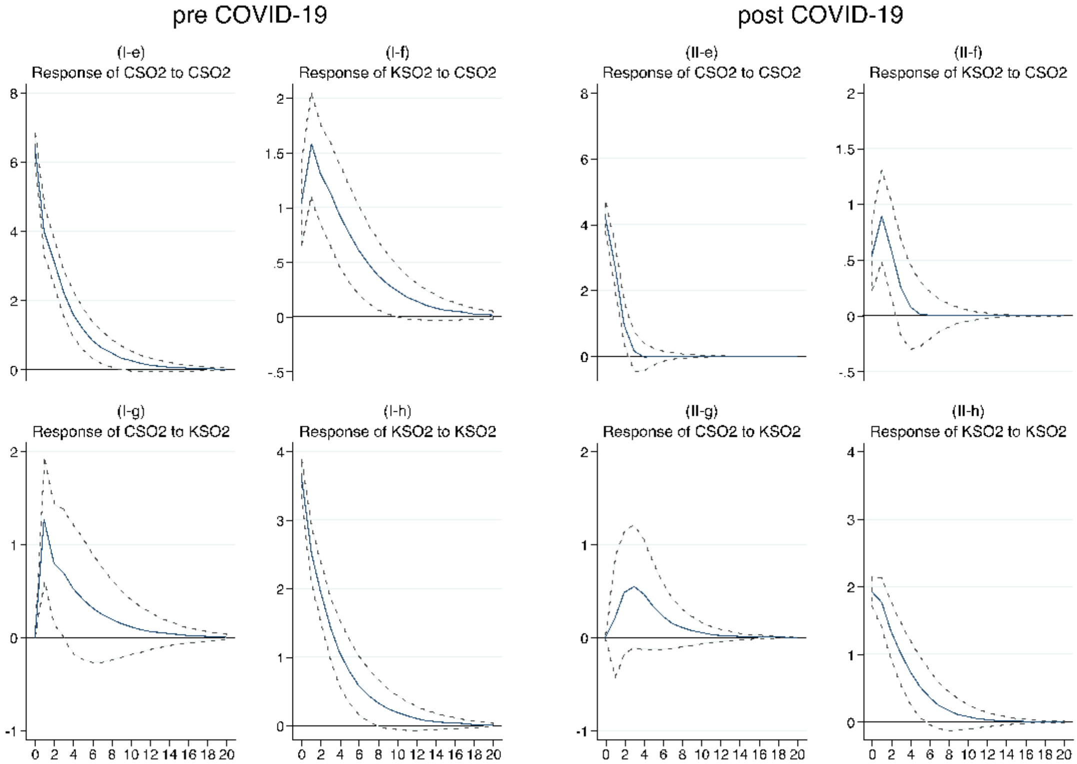


Figure 7. Impulse response of $SO_2$ concentration (μg/$m^3$)
in capital areas of China and South Korea

## References

Anjum, N.A., 2020. “Good in The Worst: COVID-19 Restrictions and Ease in Global Air Pollution," Preprints 2020, 2020040069.

Baker, S, N Bloom, S Davis and S Terry, 2020. “COVID-induced economic uncertainty and its consequence", VoxEU.org, 13 April.

Baldwin, R, Mauro, B.W., 2020. “Mitigating the COVID economic crisis: Act fast and do whatever it takes, London: CEPR Press.

Chun, Y., Boo, K., Kim, J., Park, S., Lee, M., 2001. Synopsis, transport, and physical characteristics of Asian dust in Korea, J. Geophys. Res.106 (D16).

Deb, P., Furceri, D., Ostry, J.D., Tawk, N., 2020. The Economic Effects of COVID-19 Containment Measures, International Monetary Fund Working Paper No.20/158.

He, G., Pan, Y., Tanaka, T., 2020. “COVID-19, City Lockdowns, And Air Pollution: Evidence from China," The Hong Kong University of Science and Technology, Institute for Emerging Market Studies, Working Papers No.2020-72.

Huang, Y., 2021. “The Environmental Challenges of China’s Recovery After COVID- 19,” Time, Retrieved April 8, 2021, from <https://time.com/5935138/chinas-environment-economic-recovery/>.

Jia, R., Ku, H., 2019. Is China's Pollution the Culprit for the Choking of South Korea? Evidence from the Asian Dust, The Economic Journal, 129, 624, 3154-3188.

Kim, M.J., 2019. “The effects of transboundary air pollution from China on ambient air quality in South Korea," US National Library of Medicine, National Institutes of Health, online article <https://www.ncbi.nlm.nih.gov/pmc/articles/PMC6926254/>.

Kim, S.Y., Kim, H., Lee, J.T., 2020. Health Effects of Air-Quality Regulations in Seoul Metropolitan Area: Applying Synthetic Control Method to Controlled-Interrupted Time-Series Analysis, Atmosphere, 11, 868.

Lee, D., Lee, Y., Jang, K., Yoo, C., Kang, K., Lee, J., Jung, S., Park, J., Lee, S., Han, J., Hong, J., Lee, S., 2011. Korean National Emissions Inventory System and 2007 Air Pollutant Emissions, Asian Journal of Atmospheric Environment, 5 (4), 278-291.

Ministry of the Environment of Denmark, n.d.. Other international obli- gations on the environmental front, retrieved April 8, 2021, from < <https://www2.mst.dk/udgiv/publications/1995/87-7944-324-9/html/36.htm>.

NASA, 2015. New NASA Satellite Maps Show Human Fingerprint on Global Air Quality. Retrieved April 8, 2021, from <https://www.nasa.gov/press-release/new-nasa-satellite-maps-show-human-fingerprinton-global-air-quality>.

Oh, H., Ho, C., Kim, J., Chen, D., Lee, S., Choi, Y., Chang, L., Song, C., 2015. “Long-range transport of air pollutants originating in China: A possible major cause of multi-day high-PM10 episodes during cold season in Seoul, Korea," Atmospheric Environment, Volume 109, Pages 23-30.

Sun, D., Fang, J., Sun J., 2018. Health-related benefits of air quality improvement from coal control in China: Evidence from the Jing-Jin-Ji region, Resources, Conservation and Recycling, 129, 416-423.

Urrutia-Pereira, M., Mello-da-Silva, C.A., Sole, D., 2020. “COVID-19 and air pollution: A dangerous association?" Allergologia et Immunopathologia, forthcoming.

Wang et al., 2018. “Analysis of SO2 Pollution Changes of Beijing-Tianjin-Hebei Region over China Based on OMI Observations from 2006 to 2017," Advances in Meteorology, Volume 2018, Article ID 8746068, 15 pages. Retrieved April 8, 2021, from <https://www.hindawi.com/journals/amete/2018/8746068/>.

WHO, 2020. Retrieved April 8, 2021, from <https://www.who.int/news-room/detail/29-06-2020-covidtimeline>.

World Air Report, 2019. Retrieved April 8, 2021, from

<file:///Users/yimengdu/Downloads/2019-World-Air-Report-V8-20200318.pdf>.
Xiao, Q., Ma, Z., Li, S., Liu, Y., 2015. “The Impact of Winter Heating on Air Pollution in China," Environmental Science, Medicine, PloS one.
Yim, S.H.L, Gu, Y., Shapiro, M.A, Stephens, B., 2019. “Air quality and acid deposition impacts of local emissions and transboundary air pollution in Japan and South Korea,” Atmospheric Chemistry and Physics, 19, 13309-13323.
Zhang, Q., Jiang, X., Tong, D. et al., 2017. “Transboundary health impacts of transported global air pollution and international trade,” Nature, 543, 705–709.

# Appendix.

Table A1: Estimation results on PM2.5 concentration
*Sample period: the whole year of 2019*

| | CPM2.5 | | KPM2.5 | |
|---|---|---|---|---|
| | (1) | (2) | (3) | (4) |
| L.CPM2.5 | 0.720*** | 0.707*** | 0.192*** | **0.170***** |
| | (0.055) | (0.051) | (0.027) | (0.029) |
| L2.CPM2.5 | -0.269*** | -0.264*** | -0.125*** | **-0.106***** |
| | (0.067) | (0.061) | (0.033) | (0.034) |
| L3.CPM2.5 | 0.079 | 0.024 | 0.034 | 0.020 |
| | (0.060) | (0.055) | (0.029) | (0.029) |
| L.KPM2.5 | 0.162 | 0.159 | 0.991*** | **0.927***** |
| | (0.111) | (0.102) | (0.055) | (0.059) |
| L2.KPM2.5 | 0.022 | 0.092 | -0.496*** | **-0.449***** |
| | (0.153) | (0.140) | (0.076) | (0.075) |
| L3.KPM2.5 | -0.018 | -0.022 | 0.264*** | **0.213***** |
| | (0.105) | (0.097) | (0.052) | (0.052) |
| precipitation_c | | -0.261 | | |
| | | (0.357) | | |
| wind speed_c | | -4.625*** | | |
| | | (0.596) | | |
| temperature_c | | -0.424** | | |
| | | (0.177) | | |
| precipitation_k | | | | -0.261** |
| | | | | (0.113) |
| wind speed_k | | | | -0.143 |
| | | | | (0.208) |
| temperature_k | | | | -0.356*** |
| | | | | (0.108) |
| cons | 39.47*** | 87.97*** | 8.174*** | 23.12*** |
| | (6.082) | (8.616) | (2.999) | (6.477) |
| R-squared | 0.444 | 0.540 | 0.738 | 0.752 |
| S.E.equation | 33.45 | 30.56 | 16.49 | 16.12 |
| F-statistic | 48.16 | 47.17 | 169.8 | 121.7 |
| AIC | 18.22 | 18.05 | 18.22 | 18.15 |

Note: standard errors in parentheses, * $p < 0.1$, ** $p < 0.05$, *** $p < 0.01$

Table A2: Estimation results on SO2 concentration

*Sample period: the whole year of 2019*

| | $CSO_2$ | | $KSO_2$ | |
|---|---|---|---|---|
| | (1) | (2) | (3) | (4) |
| L.$CSO_2$ | 0.566*** | 0.494*** | 0.134*** | **0.111***** |
| | (0.053) | (0.053) | (0.031) | (0.032) |
| L2.$CSO_2$ | 0.082 | 0.042 | -0.053* | **-0.080**** |
| | (0.054) | (0.053) | (0.031) | (0.033) |
| L.$KSO_2$ | 0.349*** | **0.338***** | 0.691*** | **0.678***** |
| | (0.093) | (0.089) | (0.055) | (0.054) |
| L2.$KSO_2$ | -0.221** | **-0.247***** | 0.015 | -0.005 |
| | (0.093) | (0.091) | (0.055) | (0.056) |
| precipitation_c | | -0.147** | | |
| | | (0.073) | | |
| wind speed_c | | -0.042 | | |
| | | (0.124) | | |
| temperature_c | | -0.182*** | | |
| | | (0.036) | | |
| precipitation_k | | | | 0.021 |
| | | | | (0.027) |
| wind speed_k | | | | -0.051 |
| | | | | (0.046) |
| temperature_k | | | | -0.093*** |
| | | | | (0.028) |
| cons | 3.260*** | 9.025*** | 4.098*** | 7.514*** |
| | (1.140) | (1.666) | (0.668) | (1.522) |
| R-squared | 0.516 | 0.560 | 0.623 | 0.635 |
| S.E.equation | 6.482 | 6.211 | 3.800 | 3.757 |
| F-statistic | 96.84 | 65.89 | 150.2 | 90.21 |
| AIC | 12.03 | 11.97 | 12.03 | 11.97 |

Note: standard errors in parentheses, * $p < 0.1$, ** $p < 0.05$, *** $p < 0.01$

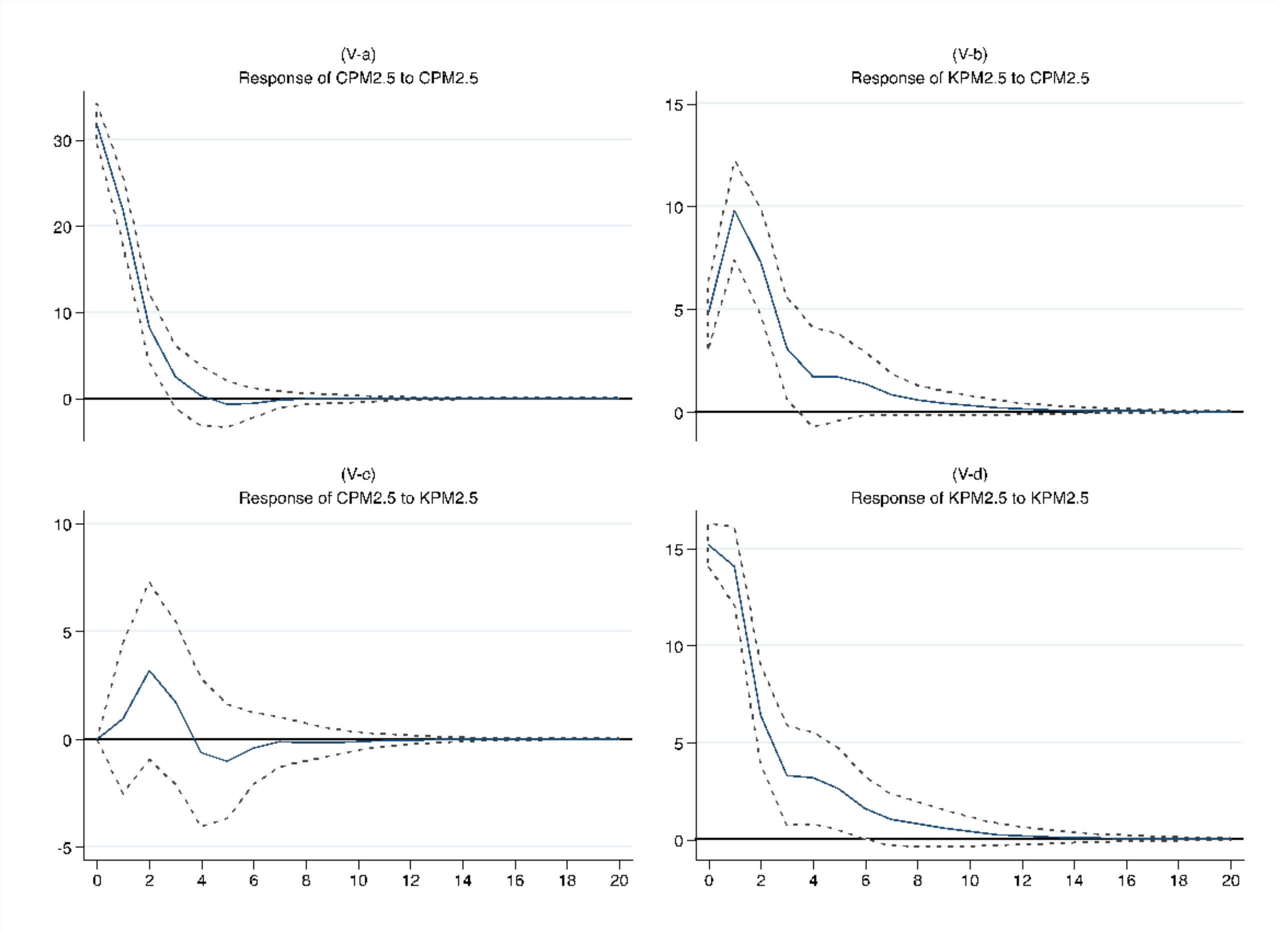


Figure A1. Impulse response of PM2.5 concentration (μg/m$^3$) in capital areas of China and South Korea, *sample period: the whole year of 2019*

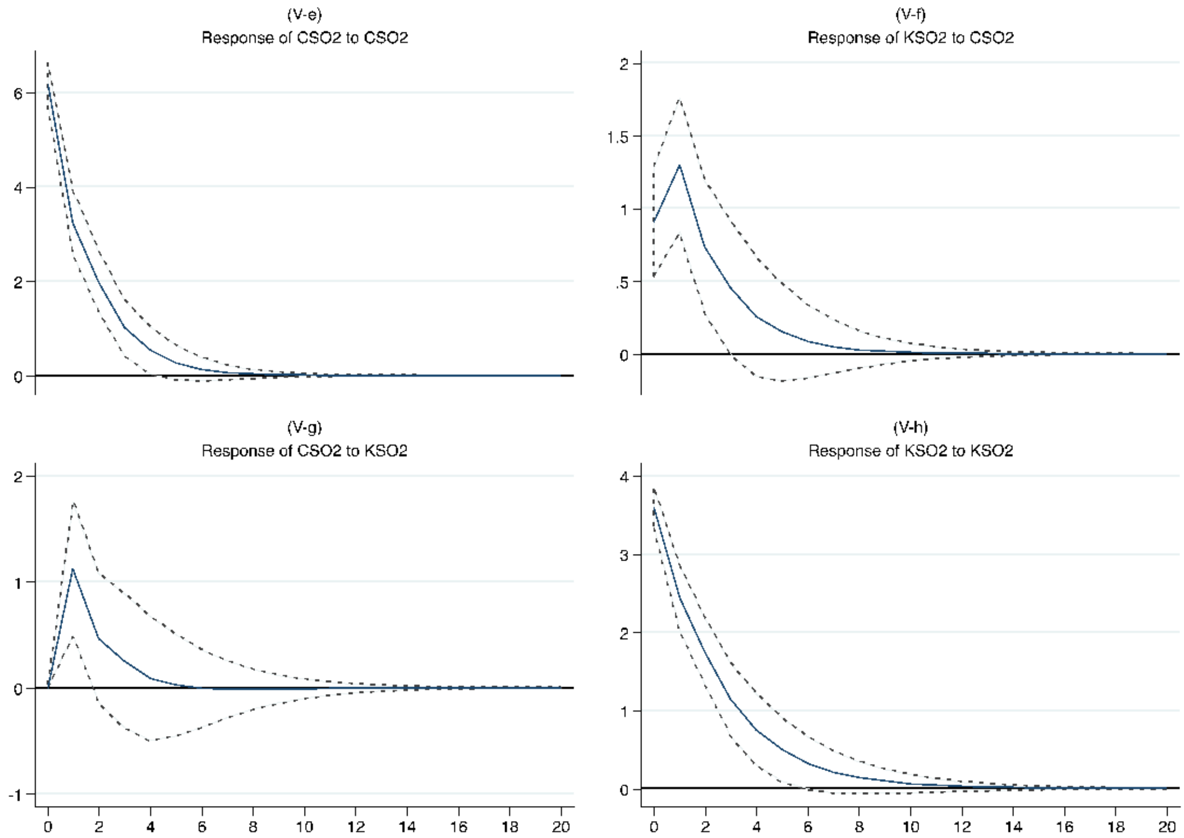


Figure A2: Impulse response of SO2 concentration (μg/m$^3$) in capital areas of China and South Korea, *sample period: the whole year of 2019*